Physics of Plasmas

Study of laser-driven magnetic fields with a continuous wave Faraday rotation diagnostic

Cite as: Phys. Plasmas **27**, 033102 (2020); https://doi.org/10.1063/1.5141753
Submitted: 06 December 2019 . Accepted: 19 February 2020 . Published Online: 03 March 2020

V. V. Ivanov, A. V. Maximov, A. L. Astanovitskiy, I. A. Begishev, R. Betti, J. R. Davies, C. Mileham, J. D. Moody, C. Stoeckl, K. J. Swanson, N. L. Wong, and J. Bromage

Physics of Plasmas ARTICLE scitation.org/journal/php

Study of laser-driven magnetic fields with a continuous wave Faraday rotation diagnostic

Cite as: Phys. Plasmas **27**, 033102 (2020); doi: 10.1063/1.5141753
Submitted: 6 December 2019 · Accepted: 19 February 2020 ·
Published Online: 3 March 2020

V. V. Ivanov,[1,a)] A. V. Maximov,[2] A. L. Astanovitskiy,[1] I. A. Begishev,[2] R. Betti,[2] J. R. Davies,[2] C. Mileham,[2] J. D. Moody,[3] C. Stoeckl,[2] K. J. Swanson,[1] N. L. Wong,[1] and J. Bromage[2]

AFFILIATIONS

[1]Department of Physics, University of Nevada, Reno, Nevada 89557, USA
[2]University of Rochester, Laboratory for Laser Energetics, New York 14623, USA
[3]Lawrence Livermore National Laboratory, Livermore, California 94550, USA

[a)]Author to whom correspondence should be addressed: ivanov@unr.edu

ABSTRACT

Magnetic fields driven by a laser in coil targets were studied for laser energies of ∼25 J and two pulse durations of 2.8 ns and 70 ps. Axial magnetic fields in the coils were measured by continuous wave Faraday rotation diagnostics. The diagnostics indicated magnetic fields of 6–14 T in the coil and currents of 10–20 kA. Magnetic fields were compared for similar laser targets, focusing conditions, and laser energies. A 30-times increase in the intensity of the laser beam by reducing the pulse duration resulted in an increase in the magnetic field and current by a factor of 2. The relaxation time of the magnetic pulse was on the sub-microsecond scale.

I. INTRODUCTION

Studies on magnetized plasma are relevant to many fields of basic and applied plasma physics and astrophysics. The compression of pre-heated magnetized plasma is a key point of the MagLIF concept for controlled fusion.[1] Strong magnetic fields can improve plasma conditions for inertial confinement fusion.[2] Magnetic fields change the dynamics of plasma expansion[3–5] and the development of instabilities in plasma.[6] Strong magnetic fields are expected to enhance the generation of ion beams.[7] Laboratory laser produced magnetized plasma can be scaled to astrophysical plasmas.[4,8]

Strong magnetic fields can be generated by kJ-class lasers using coil targets. A 0.5–2 kJ laser with a pulse duration of ∼1 ns generates laser produced plasma and fast electrons that induce a current in the coil generating a magnetic field. This method was originally demonstrated by Korobkin and Motylev in Ref. 9. Generation of magnetic fields of 50–200 T was presented in Refs.10 and 11. Higher magnetic fields of 600–800 T were reported in Refs. 12 and 13. A theory of generation of laser-driven magnetic fields was developed in Refs. 14 and 15. Strong magnetic fields of 100–300 T are also generated by 1–3 MA pulsed power machines in coil and rod loads.[3,16,17]

Measurements quantifying magnetic fields in coil targets confront several challenges. The discharge in the coil generates optical, x-ray, and radio frequency electromagnetic bursts. X-ray radiation and eddy currents can initiate plasma formation on a laser target near the coil.[16] For these reasons, magnetic probes are installed at a distance of 5–7 cm where the signal drops by a factor of 10^3–10^4.[6,13,14] Zeeman spectral splitting has been applied successfully to magnetized plasma with an electron temperature of 1–15 eV.[18] The Faraday rotation method enables the measurement of magnetic fields at the rising edge of the laser driven *B*-field.[10] Proton radiography is widely used but is sensitive to both E-fields and *B*-fields and, typically, provides one time frame in a stack of RCF films.[11,13] The characteristic rise time of the laser driven magnetic field may be < 0.5 ns. The comparison of magnetic fields in different experiments is difficult because *B*-fields are generated by lasers with different wavelengths, energies, intensities, focusing conditions, and target designs.

In this paper, generation of magnetic fields in laser coil targets was studied at pulse durations of 2.8 ns and 70 ps with a laser energy of ∼25 J at the same laser with identical focusing conditions. The intensity in the focal spot on the capacitor target was varied by a factor of ∼30. The axial magnetic field was measured by Faraday rotation of a continuous wave (CW) laser beam at the wavelength of 405 nm in a small glass disk. The Faraday diagnostics provided continuous measurements of all features of the magnetic pulse in one shot. The magnetic pulse had a short 0.3–2 ns rising edge and a sub-microsecond falling edge. The long falling edge is a result of relaxation of the magnetic energy of the coils through the capacitor shorted by the laser produced plasma.

II. EXPERIMENTAL SETUP

Experiments were carried out at the Multi-Terawatt Laser (MTW) of the Laboratory for Laser Energetics (LLE), University of Rochester. The laser is based on the OPCPA front-end and neodymium glass amplifiers.[19] The MTW laser produced pulses with durations of 70 ps (compressed) or 2.8 ns (with the compressor bypassed) at the central wavelength of 1053 nm. The beam was focused by an F/2 parabolic mirror on the inner plate of the target capacitor at an ~7 μm spot. The energy on the target for the short pulse was smaller due to the 80% transmission of the compressor, and so average intensities in the spot were 0.8×10^{16}–2.5×10^{17} W/cm^2 in the long and short pulse regimes.

Faraday rotation of the polarization plane of a CW probe laser was measured in a Tb doped glass disk, 1 mm thick and 1.5 mm in diameter. This diagnostics was developed and calibrated during measurements of magnetic fields at the Zebra pulsed power generator.[17] A Verdet constant of the Faraday glass was measured by two methods using a pulse solenoid and permanent magnets. The power of the CW laser at the wavelength of 405 nm was 150 mW. An input Glan polarizer with a contrast $>10^4$ allowed for measurements of small angles of the Faraday rotation. The beam was focused on the glass disk by the lens with a focal length $F = 2$ m. A mechanical shutter opened the laser beam during a 10 ms window to avoid heating or damaging the glass sample. The laser beam was reflected back from the dielectric mirror on the rear side of the Faraday glass disk as seen in Fig. 1(a). After the polarization plane of the laser beam has been rotated by the magnetic field, the light is reflected out of the beam path by the Glan polarizer. The depolarized part of the beam was focused onto a 7 GHz silicon photodiode and recorded using an oscilloscope. A narrowband interference filter blocked the light pulse from the plasma generated during laser irradiation. The Faraday glass disk was placed at a distance of 0.5–1.5 mm from the coil edge. A thin glass plate protected the rear dielectric mirror on the Faraday disk against plasma debris. Double disks were used in several shots to increase the Faraday rotation angle. The Faraday rotation diagnostics with a CW laser provided a continuous measurement of the magnetic field in a long temporal range.

A coil laser target was made of Cu101 foil with a 99.99% purity and 0.1 mm thick. The coil with an internal diameter of 1 mm was 1 mm wide. A laser beam passed through the 0.6 mm hole in the inner plate of the capacitor and focused on the rear plate as seen in Figs. 1(a) and 1(b). The gap between the plates was 1 mm. The coil axis was rotated 45° compared to the capacitor plane due to the configuration of windows in the interaction vacuum chamber. Coil targets were not evaporated or melted but were unbent by the plasma pressure after the laser shot.

A CW laser at 405 nm was used due to the high Verdet constant of the Faraday glass in the blue range. The back reflecting diagnostics provided a double pass of the laser beam in the Faraday glass. However, the laser signal from the photodiode was in the mV range due to the low CW laser power, small B-fields in the coil, and the decreased sensitivity of the silicon photodiode in the blue range. The oscilloscope and photodiode were placed in a screened cage to mitigate the electromagnetic noise during the laser shot.

III. GENERATION OF LASER DRIVEN MAGNETIC FIELDS AT THE MTW LASER

A. Generation of magnetic fields by the 2.8 ns laser pulse

During the first series of shots, the magnetic field in the coil target was produced by the 2.8 ns laser pulse. The laser pulse was focused on the capacitor plate with an intensity of 0.8×10^{16} W/cm^2. A pulse shape of the Faraday signal was recorded by the 7 GHz silicon photodiode on a 12 GHz oscilloscope.

A typical Faraday signal is shown in Fig. 2. The electromagnetic noise during the shot was averaged during 1 ns and 2 ns (black and red lines). Every voltage point was replaced by the value averaged in the range $\pm$ 0.5 ns or $\pm$ 1 ns. In this shot, the Faraday glass disk was placed at a distance $z = 0.45$ mm from the edge of the coil. The rotation angle α was calculated by formula $U/U_{max} = \sin^2\alpha$, where U and U_{max} are the amplitude of the signal and the maximum amplitude, respectively. The maximum amplitude U_{max} was measured in the reference alignment shots with a shutter and a quarter-wave plate installed in the beam path.

The pulse of the magnetic field generated by the nanosecond laser pulse had a 1–2 ns rising edge and a long falling edge with a submicrosecond relaxation time. The magnetic field in the glass disk was calculated from the formula for the Faraday rotation angle $\alpha = VB_{aver}l$, where V is the Verdet constant equal to $V = 171$ rad/T/m at 405 nm. The measured magnetic field B_{aver} represented the average field integrated along the length l of the Faraday glass disk. The magnetic field on the axis of the coil at the distance x was calculated using the

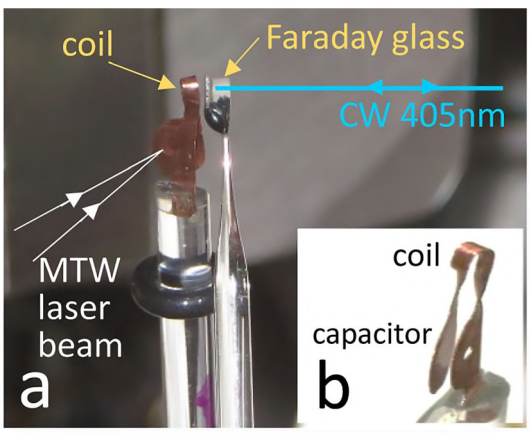

FIG. 1. (a) The laser coil target and Faraday glass disk in the MTW interaction vacuum chamber. (b) A laser coil target.

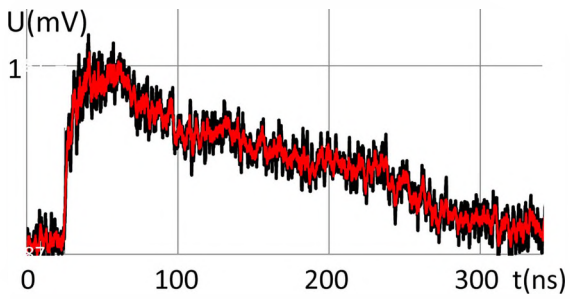

FIG. 2. A waveform of Faraday rotation signal taken at the shot with a 2.8 ns laser pulse. The noise is averaged for 1 ns (black line) and 2 ns (red line).

following formula from Ref. 20, which assumes a uniform current in the coil:,

$$B_z(x) = \frac{\mu_0 I}{4b} \cdot \left\{ \frac{b-x}{a_2-a_1} ln\left[\frac{a_2 + \sqrt{a_2^2 + (b-x)^2}}{a_1 + \sqrt{a_1^2 + (b-x)^2}} \right] + \frac{b+x}{a_2-a_1} ln\left[\frac{a_2 + \sqrt{a_2^2 + (b+x)^2}}{a_1 + \sqrt{a_1^2 + (b+x)^2}} \right] \right\}, \quad (1)$$

where a_1 and a_2 are the internal and external radii of the coil, and $2b$ is width of the coil. The inductance of the coil is $B_z(0)$ x $\pi a_1^2/I$. The total inductance of the coil and a 1 mm strip line is 0.66 nH. Figure 3 presents the position of the glass disk, the coil edge, and the axial magnetic field $B_z(x)$ calculated from formula (1). The peak magnetic field B_{aver} calculated from the Faraday signal is 0.4 T in the shot presented in Fig. 3. To reconstruct the current in the coil, the magnetic field in Fig. 3 was integrated along the disk area and the current in formula (1) was varied to fit the experimental value. A distribution of current in the coil due to the skin effect does not significantly affect calculations. Variation of the foil thickness from 0.1 mm to 0.01 mm in formula (1) results in a <5% change of $B_z(x)$ at a distance of 0.5–1.5 mm. Current may also concentrate in two layers at the ends of the coil cylinder. In this case, the axial magnetic field deviates from formula (1) by 5%–12%. The strong skin effect is more important for the rising edge as seen in the pulse shape in Fig. 2. Out calculations are performed at the maximum of the pulse where the skin effect is weak and the skin layer width is ~60 μm. The magnetic field in the coil center and the current in the coil were found to be $B_z(0) = 6.4$ T and $I_c = 9.7$ kA, respectively. The magnetic energy in the coil was 0.03 J, which is ~0.1% of the energy of the laser pulse.

B. Generation of magnetic fields by the 70 ps laser pulse

The second series of shots with coil targets were performed with a short laser pulse. A chirped laser pulse was compressed to a 70 ps duration and focused on the capacitor plate by the same focusing system with an intensity of 2.5 × 10^{17} W/cm^2. The electromagnetic noise during the short pulse shots was higher compared to that during the nanosecond shots (see Ref. 21) The noise consisted of spikes with a period of 60–120 ps. Due to the high level of the electromagnetic noise, the 12 GHz oscilloscope was changed to a better protected 2.5 GHz oscilloscope. The screen box with the photodiode and the oscilloscope were relocated at a larger distance from the interaction chamber and the MTW laser. This helped to decrease the noise and to record the sub-nanosecond rising edge of the Faraday pulse without averaging. Figure 4 shows Faraday signals from two shots with a 70 ps laser pulse recorded with (a) 12 GHz and (b) 2.5 GHz oscilloscopes. The Faraday signal in Fig. 4(a) was averaged over 1 ns (black line) and 2 ns (red line). The falling edge shows a sub-microsecond relaxation but the rising edge shorter than 1 ns cannot be resolved. Figure 4(b) presents a signal after the noise mitigation. The blue line shows the signal without averaging. The red line shows the pulse averaged for 1 ns with a sub-microsecond relaxation. The blue line in the magnified image (c) shows a 0.6 ns rising edge of the Faraday signal. The 0.5–0.6 ns front of the waveform of the Faraday pulse was typical for shots with the 70 ps laser pulse. The rising edge of the magnetic pulse is estimated as 0.3–0.4 ns if the temporal resolutions of the oscilloscope and the photodiode are taken into account.

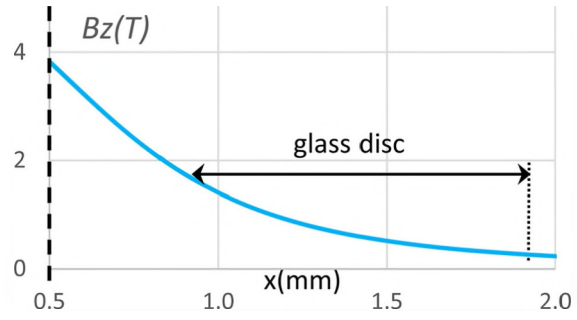

FIG. 3. The position of the glass disk and coil and the axial magnetic field $B_z(x)$ calculated by formula (1) with $I_c = 9.7$ kA. A dashed line indicates the edge of the coil.

C. Comparison of magnetic fields generated by the long and short laser pulses

Magnetic fields in both nanosecond and picosecond regimes were generated in identical conditions with the exception of the laser pulse duration and intensity. The MTW laser produced pulses with the same wavelength and spectrum using the same focusing system. The energy of the pulses was in the range of 22–26 J. The same laser coil targets were used in the nanosecond and picosecond regimes.

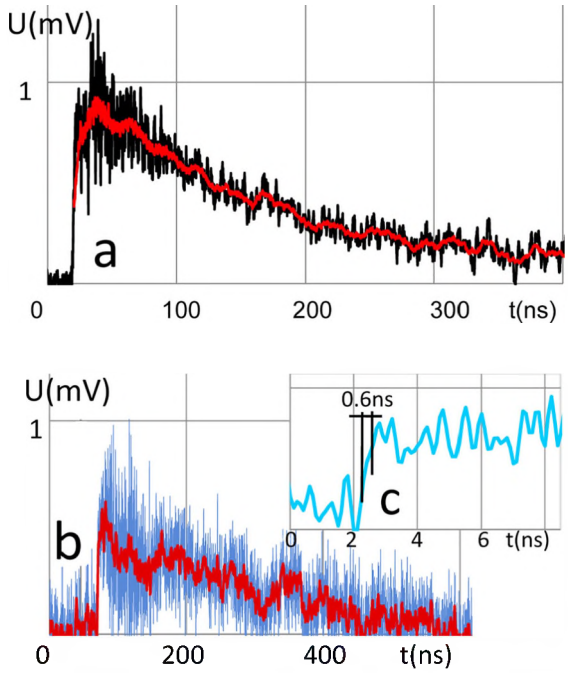

FIG. 4. Faraday signals from shots with 70 ps laser pulse with (a) 12 GHz and (b) 2.5 GHz oscilloscopes. Noise is averaged during 1 ns and 2 ns as shown by the red and black lines. Blue lines show the signal without averaging. A rising edge of the signal from image (b) without averaging is shown in (c).

Only the intensity on the capacitor plate of the laser coil was varied. Six shots with two pulse durations were performed in one series. Laser intensity in the focal spot was 0.8×10^{16} W/cm^2 for 2.8 ns pulses and 2.5×10^{17} W/cm^2 for the 70 ps pulses, so, the intensity varied by ~30 times.

The average magnetic field in the Faraday glass disk was calculated from the rotation angle. The distance between the Faraday glass disk and the coil edge was measured on every shot. Magnetic fields in the coil center and current were reconstructed from formula (1).

Figure 5 shows the current in the coil calculated from the experimental magnetic field B_{aver} in six shots. Shots with the 2.8 ns laser pulses show a current of 10.2 ± 0.7 kA. Shots with 70 ps pulses show a current of 19.8 ± 2 kA. The magnetic field is higher by a factor of 1.94 in the short pulse regime. An increase in laser intensity by a factor of ~30 results in the increase in the current in the coil and in the increase in the magnetic field by ~2 times.

IV. DISCUSSION

Experimental data were compared with models for the generation of laser driven magnetic fields. A model published in Ref. 14 estimated the current in coil targets irradiated by a laser pulse. Fast electrons from the laser produced plasma charge the capacitor of the target and drive current I_c through the coil. The charging of the capacitor and the generation of the coil current I_c are described by the following equations:[14]

$$C\frac{dU}{dt} = I_0 e^{-\frac{d}{C_s t}} - I_0 e^{\frac{U}{T_e}} + I_c, \tag{2}$$

$$-U = RI_c + L\frac{dI_c}{dt}, \tag{3}$$

where U is the voltage between the plates of the capacitor C, d is the distance between the plates, T_e is the temperature of hot electrons, C_s is the ion sound speed, and L and R are the coil inductance and resistance. The first and the second terms in the right hand side of equation (2) are the ion and electron currents flowing in the gap. The "electrotechnical" Eq. (3) describes the dynamics of coil current I_c. Similar equations with different expressions for the electron and ion currents from plasma were used in Ref. 11. However, the solution of these equations gives oscillating currents.

Let us note that the system of equations for the coil current has to describe the physics of the processes that develop on four different timescales: (1) the time interval when the laser pulse is irradiating the target; (2) the time duration of the electron current; (3) the time duration of the ion current; (4) the coil current evolution at large times due to circuit characteristics (capacitance, inductance, and resistance). Equations (2) and (3) present a basic model that accounts for the current dynamics on these 4 timescales.

Further studies of physics of laser driven currents were carried out in Ref. 15. This model did not use the ion current in the equations. It was also shown that the nanosecond relaxation of the magnetic pulse is a result of increased resistivity of the coil material due to the fast heating by the current. However, the theoretical model[15] was developed for ns pulses and cannot be applied to the 70 ps laser pulse in our experiments. The model suggests that hot plasma arrives at the anode and provides a stationary regime at ~100 ps for the laser pulse with a duration ≥1 ns. In the model,[15] the current is calculated only after 100 ps. However, experiments[22] showed that 30 fs laser pulses effectively generate the magnetic field in the coil laser target and a B-field reaches the maximum at ~60 ps.

The temperature of hot electrons in plasma is crucial for the generation of the laser driven magnetic field. Several experimental scaling laws for hot electron energy have been published for laser intensities in the range of 10^{14}–10^{19} W/cm^2.[22–24] Energy scales as $T_e \sim I^{0.25}$ in Ref. 23, $\sim I^{0.3}$ in Ref. 24, and $\sim I^{0.42}$ in Ref. 25. We scaled the temperature of hot electrons using the formula from:[15] $T_e = 12(\lambda^2 I)^{0.42}$, where T_e is in keV, the laser wavelength λ is in μm, and intensity I is in PW/cm^2. In this case, the temperature of hot electrons is 30 keV for the 2.8 ns pulse and 128 keV for the 70 ps pulse. Figure 6 presents the coil current I_c calculated from Eqs. (2) and (3) using parameters of our coil target, $d = 1$ mm, $C = 0.08$ pF, and $L = 0.66$ nH and the size of the focal spot of 8 μm. Solid and dashed lines in Fig. 6 correspond to calculations with and without the ion current, described by the first term in Eq. (2). The coil current is only ~20% higher if the ion current is not included in the calculations. However, without the ion current, Eqs. (2) and (3) do not show the fast relaxation of coil current after its maximum that agrees with our experiments. The ratio of maximum currents $I_c(128\,\text{keV})/I_c(30\,\text{keV}) = 2$ is in agreement with the experimental ratio for the short and long pulses. The maximum current and rising time of the current pulse are also in agreement with these simulations. The dotted lines show calculations with inductance increased

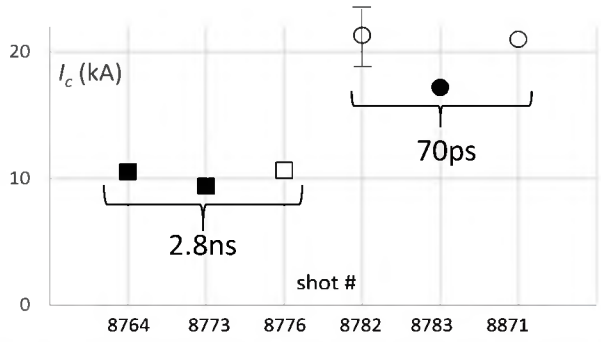

FIG. 5. Current in the coil calculated in a series of shots with 2.8 ns pulses (squares) and 70 ps pulses (circles). Filled markers show shots with single Faraday glass disks. Open markers present shots with double disks.

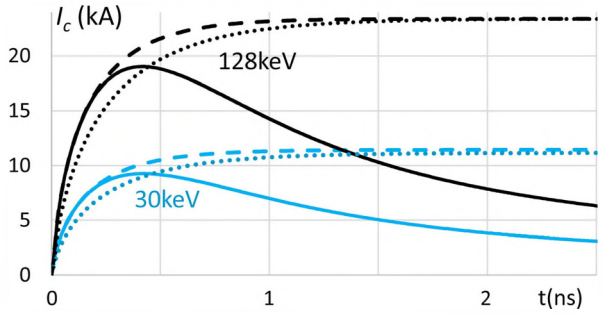

FIG. 6. Current in the coil calculated from formulas (2,3). Dashed lines show calculations without ion current in Eq. (2). The dotted lines show calculations with inductance increased by a factor of 1.5.

by a factor of 1.5. Variation of inductance in Eqs. (2) and (3) affects the rising edge but does not affect the maximum current in the coil. We note that the energy of fast electrons may vary if another scaling is used. Moreover, the model from[14] does not take into account some physics effects presented in Ref. 15, such as the effects of the space charge, magnetization, and heating of the coil material. Further experiments and theoretical efforts should be performed to better understand the physical effects responsible for the generation of the laser driven magnetic fields.

However, the experiments with laser energy at the kJ level demonstrate the nanoseconds falling edge of the magnetic pulse. The short relaxation time of the current was explained by high resistance of the coil material $\sim 1\ \Omega$ near the temperature of evaporation.[15] In our experiments, the coil was made of $1 \times 0.1\ \mathrm{mm}^2$ Cu foil with a total mass of ~5 mg. Dissipation of a magnetic energy of 0.03 J can increase coil temperatures by about ~20 K. If the skin layer is negligibly small, then the bulk resistance of the coil is $R = 2 \times 10^{-3}\ \Omega$ with the inductance $L = 0.66$ nH. The relaxation time of the magnetic energy through the coil and plasma in the gap is $L/R = 0.33\ \mu$s. This relaxation time is in agreement with the long falling edge in Figs. 2 and 4.

The rising edge of the magnetic field in the picosecond regime is 0.3 ns. The sub-nanosecond rising edge is typical for the magnetic pulse generated by kJ laser pulses.[12,13] In this case, the time rate of the magnetic field can reach the value of $dB/dt \sim 10^{12}$ T/s, and the external metal foil target will be quickly heated by eddy currents. Using the enthalpy of atomization $H_{at} = 1.2 \times 10^7$ J/kg and the resistivity $\sim 5 \times 10^{-7}\ \Omega$ at the evaporation point, one can estimate that a 1 μm aluminum foil can be evaporated during 0.2 ps. Further heating by eddy currents is balanced after 2 ps by the black body radiation at a temperature of ~4 eV. The foil expands by less than 1% of its thickness during 2 ps, and therefore, the pressure of Al plasma can reach 0.4 Mbar. However, the flashover and further heating of the surface plasma may change the heating dynamics. Dielectric targets are not heated by eddy currents but the high circular voltage may result in a flashover.

V. CONCLUSION

Laser-driven magnetic fields in coil targets were studied at the MTW laser with CW Faraday rotation diagnostics. Two pulse durations of 2.8 ns and 70 ps were used for the generation of magnetic fields. The same laser coil targets, focusing system, and laser energy were used in both nanosecond and picosecond regimes. Only the laser pulse duration and intensity on the coil target were varied in experiments. The axial magnetic fields in the coils were continuously measured by Faraday rotation of the polarization plane of the laser beam in a small glass disk placed near the coil. Faraday rotation angles indicate magnetic fields of $B = 6$–14 T in the coil center and currents of $I_c = 10$–20 kA. The 70 ps laser pulses with 30-times higher intensity compared to the 2.8 ns laser pulses generated a current and magnetic fields that were ~2 times higher. This ratio is in agreement with the simulations using equations from the model.[14] The current and the rising edge duration of the magnetic pulse were also in agreement with the model.[14]

The sub-microsecond falling edge of the magnetic pulse was observed in both laser pulse regimes. The falling edge is formed by the relaxation of the magnetic energy of the coils through the plasma-shorted capacitor. An electron-ion current in the model[14] should be presented in another form to fit the experimental relaxation time. The rising edge of the magnetic field was 1–2 ns with the 2.8 ns laser pulse and ~0.3 ns with the 70 ps laser pulse. The temporal rise of the magnetic field can reach 10^{12} T/s if a kJ laser is used. With such a rate, eddy currents can heat an external metal foil target to warm dense matter conditions.

ACKNOWLEDGMENTS

This work was supported by DOE Grant No. DE-SC0016500 and by National Science Foundation Award No. PHY-1903355 through the NSF/DOE Partnership in Basic Plasma Science and Engineering. One of the co-authors was supported by DOE Grant No. DE-SC0016258. This work was partially performed under the auspices of the U.S. Department of Energy by the Lawrence Livermore National Laboratory under Contract No. DE-AC52-07NA27344. The MTW Facility was supported by the Department of Energy National Nuclear Security Administration under Award No. DE-NA0003856.

REFERENCES

[1]A. B. Sefkow, S. A. Slutz, J. M. Koning, M. M. Marinak, K. J. Peterson, D. B. Sinars, and R. A. Vesey, Phys. Plasmas **21**, 072711 (2014).
[2]P. Y. Chang, G. Fiksel, M. Hohenberger, J. P. Knauer, R. Betti, F. J. Marshall, D. D. Meyerhofer, F. H. Seguin, and R. D. Petrasso, Phys. Rev. Letts. **107**, 035006 (2011).
[3]V. V. Ivanov, A. V. Maximov, R. Betti, P. P. Wiewior, P. Hakel, and M. E. Sherrill, Plasma Phys. Controlled Fusion **59**, 085008 (2017).
[4]B. Albertazzi, A. Ciardi, M. Nakatsutsumi, T. Vinci, J. Béard, R. Bonito, J. Billette, M. Borghesi, Z. Burkley, S. N. Chen, T. E. Cowan, T. Herrmannsdörfer, D. P. Higginson, F. Kroll, S. A. Pikuz, K. Naughton, L. Romagnani, C. Riconda, G. Revet, R. Riquier, H.-P. Schlenvoigt, I. Y. Skobelev, A. Ya. Faenov, A. Soloviev, M. Huarte-Espinosa, A. Frank, O. Portugall, H. Pépin, and J. Fuchs, Science **346**, 325 (2014).
[5]V. V. Ivanov, A. V. Maximov, R. Betti, L. S. Leal, R. C. Mancini, K. J. Swanson, I. E. Golovkin, C. J. Fontes, H. Sawada, A. B. Sefkow, and N. L. Wong, Phys. Plasmas **26**, 062707 (2019).
[6]K. Matsuo, H. Nagatomo, Z. Zhang, P. Nicolai, T. Sano, S. Sakata, S. Kojima, S. H. Lee, K. F. F. Law, Y. Arikawa, Y. Sakawa, T. Morita, Y. Kuramitsu, S. Fujioka, and H. Azechi, Phys. Rev. E **95**, 053204 (2017).
[7]A. Arefiev, T. Toncian, and G. Fiksel, New J. Phys. **18**, 105011 (2016).
[8]N. C. Woolsey, Y. Abou Ali, R. G. Evans, R. A. D. Grundy, S. J. Pestehe, P. G. Carolan, N. J. Conway, R. O. Dendy, P. Helander, K. G. McClements, J. G. Kirk, P. A. Norreys, M. M. Notley, and S. J. Rose, Phys. Plasmas **8**, 2439 (2001).
[9]V. V. Korobkin and S. L. Motylev, Sov. Tech. Phys. Lett. **5**, 474 (1979).
[10]L. Gao, H. Ji, G. Fiksel, W. Fox, M. Evans, and N. Alfonso, Phys. Plasmas **23**, 043106 (2016).
[11]C. Goyon, B. B. Pollock, D. P. Turnbull, A. Hazi, L. Divol, W. A. Farmer, D. Haberberger, J. Javedani, A. J. Johnson, A. Kemp, M. C. Levy, B. Grant Logan, D. A. Mariscal, O. L. Landen, S. Patankar, J. S. Ross, A. M. Rubenchik, G. F. Swadling, G. J. Williams, S. Fujioka, K. F. F. Law, and J. D. Moody, Phys. Rev. E **95**, 033208 (2017).
[12]J. J. Santos, M. Bailly-Grandvaux, L. Giuffrida, P. Forestier-Colleoni, S. Fujioka, Z. Zhang, P. Korneev, R. Bouillaud, S. Dorard, D. Batani, M. Chevrot, J. E. Cross, R. Crowston, J.-L. Dubois, J. Gazave, G. Gregori, E. d'Humières, S. Hulin, K. Ishihara, S. Kojima, E. Loyez, J.-R. Marquès, A. Morace, P. Nicolaï, O. Peyrusse, A. Poyé, D. Raffestin, J. Ribolzi, M. Roth, G. Schaumann, F. Serres, V. T. Tikhonchuk, P. Vacar, and N. Woolsey, New J. Phys. **17**, 083051 (2015).
[13]K. F. F. Law, M. Bailly-Grandvaux, A. Morace, S. Sakata, K. Matsuo, S. Kojima, S. Lee, X. Vaisseau, Y. Arikawa, A. Yogo, K. Kondo, Z. Zhang, C. Bellei, J. J. Santos, S. Fujioka, and H. Azechi, Appl. Phys. Lett. **108**, 091104 (2016).
[14]G. Fiksel, W. Fox, L. Gao, and H. Ji, Appl. Phys. Lett. **109**, 134103 (2016).

[15]V. T. Tikhonchuk, M. Bailly-Grandvaux, J. J. Santos, and A. Poyé, Phys. Rev. E **96**, 023202 (2017).
[16]K. Nakao, F. Herlach, T. Goto, S. Takeyama, T. Sakakibara, and N. Miura, J. Phys. E **18**, 1018 (1985).
[17]V. V. Ivanov, K. J. Swanson, G. S. Sarkisov, A. V. Maximov, P. P. Wiewior, A. L. Astanovitskiy, V. Nalajala, O. Chalyy, O. Dmitriev, and N. L. Wong, Phys. Plasmas **24**, 112707 (2017).
[18]M. R. Gomez, S. B. Hansen, K. J. Peterson, D. E. Bliss, A. L. Carlson, D. C. Lamppa, D. G. Schroen, and G. A. Rochau, Rev. Sci. Instrum. **85**, 11E609 (2014).
[19]V. Bagnoud, I. A. Begishev, M. J. Guardalben, J. Puth, and J. D. Zuegel, Opt. Lett. **30**, 1843 (2005).
[20]K. W. Struve, J. L. Porter, and D. C. Rovang, "Megagauss field generation for high-energy-density plasma science experiments," Sandia Report No. SAND2008-7015 (2008).
[21]A. Poye, S. Hulin, M. Bailly-Grandvaux, J.-L. Dubois, J. Ribolzi, D. Raffestin, M. Bardon, F. Lubrano-Lavaderci, E. D'Humières, J. J. Santos, P. Nicola, and V. Tikhonchuk, Phys. Rev E **91**, 043106 (2015).
[22]W. Wang, H. Cai, J. Teng, J. Chen, S. He, L. Shan, F. Lu, Y. Wu, B. Zhang, W. Hong, B. Bi, F. Zhang, D. Liu, F. Xue, B. Li, H. Liu, W. He, J. Jiao, K. Dong, F. Zhang, Y. He, B. Cui, N. Xie, Z. Yuan, C. Tian, X. Wang, K. Zhou, Z. Deng, Z. Zhang, W. Zhou, L. Cao, B. Zhang, S. Zhu, X. He, and Y. Gu, Phys. Plasmas **25**, 083111 (2018).
[23]D. W. Forslund, J. M. Kindel, and K. Lee, Phys. Rev. Lett. **39**, 284 (1977).
[24]F. N. Beg, A. R. Bell, A. E. Dangor, C. N. Danson, A. P. Fews, M. E. Glinsky, B. A. Hammel, P. Lee, P. A. Norreys, and M. Tatarakis, Phys. Plasmas **4**, 447 (1997).
[25]W. Priedhorsky, D. Lier, R. Day, and D. Gerke, Phys. Rev. Lett. **47**, 1661 (1981).